Antiphase synchronization in multiplex networks with attractive and repulsive interactions

Sayantan Nag Chowdhury [1], Sarbendu Rakshit,[1] Javier M. Buldú [2,3,4] Dibakar Ghosh [1,*] and Chittaranjan Hens [1,†]

[1]*Physics and Applied Mathematics Unit, Indian Statistical Institute, 203 B. T. Road, Kolkata-700108, India*
[2]*Laboratory of Biological Networks, Center for Biomedical Technology-UPM, Madrid 28223, Spain*
[3]*Complex Systems Group and GISC, Universidad Rey Juan Carlos, Móstoles 28933, Spain*
[4]*Unmanned Systems Research Institute, Northwestern Polytechnical University, Xi'an 710072, China*

A series of recent publications, within the framework of network science, have focused on the coexistence of mixed attractive and repulsive (excitatory and inhibitory) interactions among the units within the same system, motivated by the analogies with spin glasses as well as to neural networks, or ecological systems. However, most of these investigations have been restricted to single layer networks, requiring further analysis of the complex dynamics and particular equilibrium states that emerge in multilayer configurations. This article investigates the synchronization properties of dynamical systems connected through multiplex architectures in the presence of attractive intralayer and repulsive interlayer connections. This setting enables the emergence of antisynchronization, i.e., intralayer synchronization coexisting with antiphase dynamics between coupled systems of different layers. We demonstrate the existence of a transition from interlayer antisynchronization to antiphase synchrony in any connected bipartite multiplex architecture when the repulsive coupling is introduced through any spanning tree of a single layer. We identify, analytically, the required graph topologies for interlayer antisynchronization and its interplay with intralayer and antiphase synchronization. Next, we analytically derive the invariance of intralayer synchronization manifold and calculate the attractor size of each oscillator exhibiting interlayer antisynchronization together with intralayer synchronization. The necessary conditions for the existence of interlayer antisynchronization along with intralayer synchronization are given and numerically validated by considering Stuart-Landau oscillators. Finally, we also analytically derive the local stability condition of the interlayer antisynchronization state using the master stability function approach.

I. INTRODUCTION

The analysis of multilayer networks [1–6] is one of the most prosperous research lines in the last decade of network science, having more appropriate description of real-life systems than isolated networks. There are several relevant and unexpected characteristics displayed in multilayer networks, which cannot be generalized to single layer networks. Multilayer networks have enormous applications in a plethora of different contexts, including congestion of traffic [7,8], evolutionary game dynamics [9,10], extreme events [11,12], epidemic spreading processes [13–15], percolation [16,17], to name but a few. Mathematically, a multilayer network is defined as a pair $\mathcal{M} = (\mathcal{G}, \mathcal{C})$, where $\mathcal{G} = \cup_{\alpha=1}^{M} G_\alpha$ is a family of graphs $G_\alpha = (Y_\alpha, E_\alpha)$, each one representing the layer α and $\mathcal{C} = \{E_{\alpha\beta} \subseteq Y_\alpha \times Y_\beta, \ \alpha \neq \beta, \ \alpha, \beta \in \{1, 2, \ldots, M\}\}$ is the set of interlinks between nodes of different layers G_α and G_β, with $\alpha \neq \beta$. The elements of each E_α are called intralayer links of G_α. If each layer has the same set of nodes and a node is only interconnected to its counterpart replica node in the rest of the layers, i.e., $Y_1 = Y_2 = \cdots = Y_M = Y$ and

$E_{\alpha\beta} = \{(y, y) : y \in Y\}$ for every $1 \leqslant \alpha \neq \beta \leqslant M$, then this particular type of network is known as *multiplex network* [5].

The increasing availability of numerical data and the development of new techniques to characterize networks encouraged a relatively large body of researches to study the collective behavior of multilayer networks. Among all of them, synchronization [18–21] is the collective dynamical process that has captured the most attention, probably due to its prevalence in a diversity of real systems.

Several types of synchronization have been studied in the multilayer network formulation, such as breathing synchronization [22], chimera states [23–25], solitary states [26], explosive synchronization [27–29], intralayer synchronization [30–32], interlayer synchronization [33–35], relay synchronization [36], cluster synchronization [37], and many more. However, antiphase synchronous states in multilayer networks have not gained their well deserved attention.

Antiphase synchronization has been observed in many real situations such as sleep [38], resting state [39], or attentional tasks [40,41]. It is also essential in spontaneous corticocortical communication dynamics, as reported in Refs. [42,43]. From the perspective of dynamical systems, time delay and modularity have been demonstrated to induce antiphase patterns due to noise-driven transitions between different synchronization clusters [44]. Recently, antiphase collective synchronization was observed in two weakly coupled groups of

*diba.ghosh@gmail.com
†chittaranjanhens@gmail.com

electrochemical oscillators [45]. More recently, antiphase synchronous states have been observed in limit cycle oscillators, when two types of interactions, viz., attractive and repulsive coupling, coexist in a network [46]. Under this framework, a universal rule based on the collective behavior of the dynamical states was proposed for attractive-repulsively coupled limit cycle oscillators to identify the bipartiteness of a network [46]. Coexisting attractive-repulsive interactions may lead to several collective nontrivial phenomena [47–56] ranging from extreme events [57,58], solitary states [59], to chimera states [60,61], and many more.

In this paper, we explore the emergence of antiphase states in multiplex networks under the accumulated effect of attractive-repulsive interactions. Initially, the interlayer connections are solely repulsively coupled, while the rest of the intralayer connections are attractive. This setup allows the appearance of antisynchronization, consisting on the combination of intralayer synchronization (of systems within the same layer) with antiphase synchronization of oscillators of different layers. We use the master stability function approach to prove the existence of such a synchronization by adequately adjusting the interlayer and intralayer coupling functions. To validate these claims, we carry our numerical simulations of multiplex networks containing Stuart-Landau (SL) oscillator [62]. Furthermore, we obtain an analytical expression that relates the amplitude of SL oscillators at the synchronous state with the interlayer coupling strength. This relation agrees excellently with our numerical experiments for repulsive interlayer coupling strength. Apart from the identification of such mixed state (interlayer antisynchronization and intralayer complete synchronization), we also establish, with theoretical and numerical simulations, that if intralayer synchronization is possible in a multiplex network, then an interlayer antisynchronous state is always possible in that network under suitable choices of the dynamical system and the coupling functions.

Finally, we made suitable modifications of the attractive-repulsive links such that antiphase states within immediate neighbors appear in the network. When a spanning tree of any layer is replaced by repulsive links of adequate strength, we observe a transition from a mixed state to antiphase synchronization of adjacent node. Furthermore, if the multiplex network is bipartite, repulsive links added into the spanning tree enable antiphase states of the whole network. This phenomenon is analyzed theoretically with the help of graph theory. The nontrivial occurrence of antiphase synchronization in bipartite multiplex networks, by introducing repulsive couplings through a spanning tree of any layer, allows us to propose a controlling scheme. A series of numerical results in different multiplex networks show the practical applications of our analytical results.

The article is organized as follows: Section II summarizes the mathematical model of the proposed multiplex networks. Here, we include definitions of different synchronized states that will accompany the rest of our discussion. The analytical condition for interlayer antisynchronization accompanying intralayer synchronization and antiphase synchronization is represented thoroughly in Sec. III. The required network architecture for interlayer antisynchronization together with intralayer synchronization and antiphase synchronization is

derived. Section IV is devoted to numerical results on different multiplex networks. The functional relation between the SL oscillator's amplitude and interlayer coupling strength is also calculated. Lastly, Sec. V provides a discussion of our findings. In the Appendix, we analytically derived the conditions for the stability of interlayer antisynchronization and carried out numerical simulations to validate them.

II. MATHEMATICAL MODEL OF MULTIPLEX NETWORKS AND DEFINITION OF DIFFERENT EMERGENT SYNCHRONIZED STATES

Initially, we consider a bilayer (i.e., two layers) multiplex network, which is the simplest multilayer network. Each of the two undirected connected layers is composed of N nodes, which are d-dimensional identical dynamical systems. The dynamical states of the two layers are represented by the vectors $\mathbf{X}_1 = \{\mathbf{x}_{1,1}, \mathbf{x}_{1,2}, \ldots, \mathbf{x}_{1,N}\}$ and $\mathbf{X}_2 = \{\mathbf{x}_{2,1}, \mathbf{x}_{2,2}, \ldots, \mathbf{x}_{2,N}\}$, where $\mathbf{x}_{\alpha,i} \in \mathbb{R}^d$ for all $\alpha = 1, 2$ and $i = 1, 2, \ldots, N$. For this bilayer multiplex network, the intralayer adjacency matrix of the αth layer is represented by $\mathscr{A}^{[\alpha]}$, with $\alpha = 1, 2$. Furthermore, layers are connected through a set of N interlayer links, connecting nodes $\mathbf{x}_{1,i}$ and $\mathbf{x}_{2,i}$. We call the ith nodes of each layer as the replicas of node i. The evolution of the state $\mathbf{x}_{\alpha,i}$ of ith node in the layer α is given by

$$\dot{\mathbf{x}}_{1,i} = f(\mathbf{x}_{1,i}) + \epsilon \sum_{j=1}^{N} \mathscr{A}_{ij}^{[1]} G[\mathbf{x}_{1,j}, \mathbf{x}_{1,i}] + \eta H[\mathbf{x}_{2,i}, \mathbf{x}_{1,i}],$$

$$\dot{\mathbf{x}}_{2,i} = f(\mathbf{x}_{2,i}) + \epsilon \sum_{j=1}^{N} \mathscr{A}_{ij}^{[2]} G[\mathbf{x}_{2,j}, \mathbf{x}_{2,i}] + \eta H[\mathbf{x}_{1,i}, \mathbf{x}_{2,i}]. \quad (1)$$

The dynamics of each individual oscillator is governed by the vector field $f : \mathbb{R}^d \to \mathbb{R}^d$, which is continuously differentiable with respect to its argument. Here, $H : \mathbb{R}^d \times \mathbb{R}^d \to \mathbb{R}^d$ represents the coupling vectorial function between the layers and $G : \mathbb{R}^d \times \mathbb{R}^d \to \mathbb{R}^d$ is the coupling vectorial function within the layers. The parameter ϵ is the intralayer coupling strength which controls the interaction between the nodes in each layer. The interlayer coupling strength η accounts for the bidirectional coupling between the layers.

The multiplex network (1) is said to be in *intralayer synchronization*, if the dynamical units evolve synchronously within each layer. Mathematically, for the first layer, and for every $\delta_1 > 0$, there exists $\mathbf{x}_1(t) \in \mathbb{R}^d$ such that $||\mathbf{x}_{1,i}(t) - \mathbf{x}_1(t)|| < \delta_1$ as $t \to \infty$ for all $i = 1, 2, \ldots, N$. Similarly, for the second layer, and for every $\delta_2 > 0$, there exists $\mathbf{x}_2(t) \in \mathbb{R}^d$ such that $||\mathbf{x}_{2,i}(t) - \mathbf{x}_2(t)|| < \delta_2$ as $t \to \infty$ for all $i = 1, 2, \ldots, N$. Here, $(\mathbf{x}_1(t), \mathbf{x}_2(t))$ is called intralayer synchronization manifold.

On the other hand, *interlayer antisynchronization* state refers to the situation where each pair of replica nodes have exactly the same amplitude with phase difference of π. Thus, the trajectories $\mathbf{x}_{1,i}(t)$ and $\mathbf{x}_{2,i}(t)$ satisfy the relation $\mathbf{x}_{1,i}(t) + \mathbf{x}_{2,i}(t) = \mathbf{0}, \forall i = 1, 2, \ldots, N$.

Also note that *antiphase synchronization* refers to the scenario where the phase difference among two adjacent vertices is π. To measure the existence of antiphase synchronized state in the multiplex network, we propose the use of the index

TABLE I. Physical interpretation of measures for evaluating phase and synchronization dynamics.

Numerical values of measures	Dynamical states
$F_{\text{Replica}} = 0$	Interlayer antiphase synchronization
$F_{\text{Replica}} = 2$	Interlayer in-phase synchronization
$F_{\text{Layer}\alpha} = 2$	Intralayer in-phase synchronization of αth layer
$F_{\text{Layer}\alpha} = 0$	Antiphase synchronization of αth layer
$F = 0$	Antiphase synchronization of the multiplex network
$F = 2$	In-phase synchronization of the multiplex network
$\mathbf{x}_{1,i}(t) + \mathbf{x}_{2,i}(t) = \mathbf{0}, \forall i = 1, 2, \ldots, N$	Interlayer antisynchronization
$\mathbf{x}_{\alpha,i}(t) \to \mathbf{x}_\alpha(t)(\alpha = 1, 2), \forall i = 1, 2, \ldots, N$	Intralayer synchronization

$F = \langle \frac{1}{L} \sum_{i<j} \mathscr{A}_{ij}[1 + \cos(\theta_i - \theta_j)]\rangle_t$, where θ is the intrinsic phase of each oscillator [46]. Here, $\mathscr{A}_{ij}$ are the elements of the adjacency matrix of the multiplex network given by

$$\mathscr{A} = \begin{pmatrix} \mathscr{A}^{[1]} & I \\ I & \mathscr{A}^{[2]} \end{pmatrix}, \quad (2)$$

I is the identity matrix of order N. L is the total number of links defined by $L = \frac{1}{2} \sum_{i=1}^{N} \sum_{j=1}^{N} \mathscr{A}_{ij}$. Clearly, antiphase synchronization can be uniquely determined by $F = 0$.

To measure the *layerwise antiphase synchronization*, we define

$$F_{\text{Layer}\alpha} = \left\langle \frac{1}{L_\alpha} \sum_{i<j} \mathscr{A}_{ij}^{[\alpha]}[1 + \cos(\theta_{\alpha,i} - \theta_{\alpha,j})] \right\rangle_t. \quad (3)$$

Here, $L_\alpha = \frac{1}{2} \sum_{i=1}^{N} \sum_{j=1}^{N} \mathscr{A}_{ij}^{[\alpha]}$ is the total number of links of the adjacency matrix $\mathscr{A}^{[\alpha]}$ of the αth layer, and $\langle \cdot \rangle_t$ stands for time average. When $F_{\text{Layer}\alpha} = 0$, then the αth layer oscillates in antiphase synchrony state.

The *interlayer antiphase synchronized state* is defined as a state where the instantaneous phase difference between each replica of node i is π, i.e., $|\theta_{1,i}(t) - \theta_{2,i}(t)| = \pi \ \forall i = 1, 2, \ldots, N$. Here, $\theta_{\alpha,i}(t)$ is the intrinsic phase of the state $\mathbf{x}_{\alpha,i}(t)$ situated at the ith node of αth layer for $\alpha = 1, 2$. However, the phase of the nodes within a layer may or may not be correlated. To characterize this state for bilayer multiplex network, we introduce $F_{\text{Replica}} = \langle \frac{1}{N} \sum_{i=1}^{N}[1 + \cos(\theta_{1,i} - \theta_{2,i})]\rangle_t$. Note that we divide by N as their are N interlinks contributing to F_{Replica} in a bilayer multiplex network. In this way, F_{Replica} lies between 0 and 2, with $F_{\text{Replica}} = 0$ implying $|\theta_{1,i}(t) - \theta_{2,i}(t)| = \pi$ for all $i = 1, 2, \ldots, N$, i.e., interlayer antiphase synchronization state.

When phases of all nodes are equal, the system is said to be in the *in-phase synchrony state*. As per our proposed measure, $F = 2$ reflects in-phase synchronization and $F_{\text{Layer}\alpha} = 2$ signifies in-phase synchrony of the αth layer. When $F_{\text{Layer}\alpha} = 2$ holds for all α layers, we call this state *intralayer in-phase synchronization*.

We summarize all measures evaluating these emerging dynamical states in Table I. The different states of the multiplex network occur when the individual oscillators are appropriately coupled through intralayer and interlayer coupling functions. In Sec. III, we focus on understanding theoretically the role of network structure and coupling functions to perceive these types of emergent dynamical states.

III. ANALYTICAL RESULTS

A. Necessary condition for intralayer synchronization

Now, we derive the necessary condition for the intralayer synchronization state for the multiplex network (1). Suppose, intralayer synchronization occurs in all layers. Then, all trajectories $\mathbf{x}_{1,i}(t)$ of the first layer converge to $\mathbf{x}_1(t)$ at some time $t = t_1$. Similarly, all trajectories $\mathbf{x}_{2,i}(t)$ of the second layer converge to $\mathbf{x}_2(t)$ at some time $t = t_2$. Let $t_0 = \max\{t_1, t_2\}$. Then, for $t \geqslant t_0$, the rate of changes of all state variables in all respective layers should be identical. Thus, for any two arbitrary distinct generic nodes k and l in layer 1, we have $\dot{\mathbf{x}}_{1,k} = \dot{\mathbf{x}}_{1,l}$. This yields, from Eq. (1),

$$\sum_{j=1}^{N} \left(\mathscr{A}_{kj}^{[1]} - \mathscr{A}_{lj}^{[1]} \right) G[\mathbf{x}_1, \mathbf{x}_1] = 0. \quad (4)$$

A similar analysis from Eq. (1) for layer 2 immediately implies

$$\sum_{j=1}^{N} \left(\mathscr{A}_{kj}^{[2]} - \mathscr{A}_{lj}^{[2]} \right) G[\mathbf{x}_2, \mathbf{x}_2] = 0. \quad (5)$$

Therefore, to maintain the identical rate of change of all the state variables in each individual layer, we must have, for $\alpha = 1, 2$,

$$\sum_{j=1}^{N} \mathscr{A}_{kj}^{[\alpha]} = \sum_{j=1}^{N} \mathscr{A}_{lj}^{[\alpha]}, \quad \text{or} \quad G[\mathbf{x}_1, \mathbf{x}_1] = 0,$$
$$\text{or} \quad G[\mathbf{x}_2, \mathbf{x}_2] = 0. \quad (6)$$

Now, $\sum_{j=1}^{N} \mathscr{A}_{kj}^{[\alpha]} = \sum_{j=1}^{N} \mathscr{A}_{lj}^{[\alpha]}$ implies that the in-degree of each node in αth layer is equal. Importantly, all networks considered in our analysis are undirected (i.e., links are bidirectional). Thus, in-degree is here just the degree of the node and, hence, the condition implies each node in αth layer has the same number of neighbors. Therefore, the network considered in each layer is regular.

On the other hand, $G[\mathbf{x}_1, \mathbf{x}_1] = 0$ and $G[\mathbf{x}_2, \mathbf{x}_2] = 0$ together imply the intralayer coupling function G should vanish after achieving the intralayer synchronization state. Thus, for the multiplex network, the intralayer synchronization is possible, if either each of the undirected intralayer network is a regular graph or the intralayer coupling function G vanishes after achieving the intralayer synchronization state.

B. Necessary condition for interlayer antisynchronization together with intralayer synchronization

Next, we derive the necessary condition for interlayer antisynchronization state along with intralayer synchronization. First, we assume that $G[\mathbf{x}_1, \mathbf{x}_1] = 0$ and $G[\mathbf{x}_2, \mathbf{x}_2] = 0$ hold for our chosen intralayer coupling function G, which is one of the necessary condition (6) for intralayer synchronization. So, when the intralayer synchronization occurs, then Eqs. (1) reduce to

$$\dot{\mathbf{x}}_1 = f(\mathbf{x}_1) + \eta H[\mathbf{x}_2, \mathbf{x}_1], \quad \dot{\mathbf{x}}_2 = f(\mathbf{x}_2) + \eta H[\mathbf{x}_1, \mathbf{x}_2]. \quad (7)$$

Further, when interlayer antisynchronization occurs, the trajectories given by Eq. (7) approach to the interlayer antisynchronization manifold $\mathcal{M} = \{(\mathbf{x}_1, \mathbf{x}_2) : \mathbf{x}_1(t) = -\mathbf{x}_2(t) = \mathbf{x}_0(t)\}$ as time t goes to infinity. The general form of Eq. (7) reduces to

$$\dot{\mathbf{x}}_0 = f(\mathbf{x}_0) + \eta H[-\mathbf{x}_0, \mathbf{x}_0], \quad -\dot{\mathbf{x}}_0 = f(-\mathbf{x}_0) + \eta H[\mathbf{x}_0, -\mathbf{x}_0]. \quad (8)$$

These equations are consistent and compatible if and only if $f(\mathbf{x}) = -f(-\mathbf{x})$ and $H[-\mathbf{x}, \mathbf{x}] = -H[\mathbf{x}, -\mathbf{x}]$. Thus, the function $f(x)$ is an odd function of x and the intercoupling function $H(x)$ is also an odd function of x, which are the necessary conditions for interlayer antisynchronization along with intralayer synchronization. Hence, the interlayer antisynchronization along with intralayer synchronization is possible if the function $f(x)$ and the intercoupling function $H(x)$ are odd functions of x.

C. Necessary and sufficient condition for antiphase synchronization

Now, we turn our attention to the network structure, described by the adjacency matrix $\mathscr{A}$, and its relation with the antiphase synchronization state. If the system possesses antiphase synchronization, then $|\theta_i - \theta_j| = \pi$, if $\mathscr{A}_{ij} = 1$. Physically, this implies the phase differences between two adjacent nodes are π. This definition allows us to apply an isometric translation of origin in the (r, θ) plane without changing the directions of the axes, so that we can partition the entire set of vertices of the graph G associated with the adjacency matrix $\mathscr{A}$ into two disjoint sets U and V. Without any loss of generality, we can assign those nodes into the set U, which has phase 0 under the isometric translation and those nodes into the set V, which has the translated phase π. Thus, the entire graph G has exactly two phases. Let us consider a bijection ϕ from the set of distinct phases $X = \{0, \pi\}$ to $Y = \{$a set of distinct colors$\}$, such that for each unique phase of X, we assign a unique color from Y. Then, as G has exactly two distinct phases, thus the graph G requires two different colors for its proper coloring, and no less. Thus, G is 2-chromatic. Since, every 2-chromatic graph is bipartite and every bipartite graph is 2-chromatic [63], hence, G must be bipartite in nature.

The above argument trivially shows that if G is a bipartite graph, then the antiphase synchronous solution is always possible for a suitable choice of other parameters. If G is not a bipartite graph, then G is not 2-chromatic. Also, the connected graph G is not 1-chromatic, as a 1-chromatic graph represents a graph consisting of only isolated vertices. So, the graph

G is at least 3-chromatic. Again, by considering the inverse mapping ϕ^{-1}, we easily obtain at least three distinct phases of G, which is against the antiphase synchronous manifold. Hence, we can conclude that *antiphase synchronization is possible if and only if the connected graph G associated with an adjacency matrix $\mathscr{A}$ that is bipartite in nature*.

D. Obtaining antiphase synchronization using a spanning tree

Now, we discuss why *antiphase synchronization is possible for a connected graph with appropriate parameters, if the adequate coupling strength is considered through the branches of a spanning tree*. Let G be a connected graph with $N \geqslant 2$ nodes. Then, $\exists$ at least a spanning tree T of G. Note that every tree with two or more vertices is 2-chromatic. So, we can properly color T with two colors. Now, considering the same bijection ϕ^{-1} from $Y = \{$a set of distinct colors$\}$ to the set of distinct phases $X = \{0, \pi\}$, such that for each unique color from Y, we assign a unique phase of X. Since antiphase synchronization is possible, so G must be bipartite in nature as per our previous discussion. Therefore, G contains no circuits of odd length. Now, we add the chords to T one by one. Clearly, the end vertices of every chord being replaced with different phase in T. Thus, G has two distinct phases with no adjacent vertices having the same phase. Therefore, adjusting the coupling of the spanning tree, antiphase synchronization is possible depending on the other suitable ingredients like the structure of the network, the vector field of the system evolution, and the vectorial function within the layers and between the layers.

E. Required graph architecture for interlayer antisynchronization along with intralayer synchronization

When intralayer synchronization occurs, then Eqs. (7) hold, which do not contain the adjacency matrices $\mathscr{A}^{[1]}$ and $\mathscr{A}^{[2]}$. As demonstrated above, intralayer synchronization requires that either each of the undirected intralayer network is a regular graph or the intralayer coupling function G vanishes after achieving the intralayer synchronization state. Thus, when the intralayer synchrony occurs, each layer follows a single trajectory. Hence, each layer can be described by the single trajectory of any single node of that layer. The intralayer synchronization occurs in each layer simultaneously [64]. Under these circumstances, the analysis of the entire multiplex is transformed into the analysis of a chain of two nodes, where each node exhibits a trajectory representing the corresponding layer. As per our earlier discussion, for antiphase synchronization, a bipartite graph is needed. Since, a chain of two nodes is always 2-chromatic and thus, bipartite, hence under suitable choices of other parameters and dynamical systems, *interlayer antisynchronization along with intralayer synchronization is possible for any connected graph in multiplex network, if intralayer synchronization is possible in that multiplex network*.

F. Required graph architecture for antiphase synchronization in multiplex network

We already know that antiphase synchronization is possible if and only if the graph G associated with the adjacency matrix

$\mathscr{A}$ is bipartite. Hence, *antiphase synchronization is possible in a connected bilayer multiplex network, if and only if the multiplex network is bipartite in nature.* Thus, the set of nodes W of the connected graph G is partitioned into two disjoint sets U and V, such that $U \cap V = \emptyset$. Since G is bipartite, then any proper subset of W is at most 2-chromatic. Thus, the set of vertices of layer 1 associated with $\mathscr{A}^{[1]}$ is at most 2-chromatic and can be decomposed to U_1 and V_1 such that $U_1 \cap V_1 = \emptyset$ and $W_1 = U_1 \cup V_1 \subset U \cup V = W$. Similarly, the layer 2 is decomposed into U_2 and V_2 such that $U_2 \cap V_2 = \emptyset$ and $W_2 = U_2 \cup V_2 \subset U \cup V = W$. Note that U_1, U_2, V_1, and V_2 are nonempty. If any of these sets is empty, then that layer of $N \geqslant 2$ vertices would contain isolated nodes, which would be a contradiction to the connectedness of the layers of the graph G. Hence, *the graphs in both the connected layers are bipartite.*

If the connected multiplex network is a bipartite graph, then the connected layers are also bipartite in nature. But, the converse may not be true. Even if all layers are bipartite in nature, it is not guaranteed that the whole multiplex network is a bipartite graph.

IV. NUMERICAL RESULTS

In this section, we use Stuart-Landau (SL) oscillators to show some examples of our analytical results in multiplex networks of different structures. Also, the intralayer and interlayer coupling functions are adopted as $G(\mathbf{x}_i, \mathbf{x}_j) = H(\mathbf{x}_i, \mathbf{x}_j) = [x_j - x_i, y_j - y_i]^{Tr}$, where Tr denotes the transpose of a vector. All the simulations are done using the fifth-order Runge-Kutta-Fehlberg method with a fixed time step $h = 0.01$. The measures F_{Layer1}, F_{Layer2}, F_{Replica}, and F are averaged over 0.5×10^5 steps after the initial transients of 1.5×10^5 steps. The dynamics of the ith SL oscillator is represented by

$$f(\mathbf{x}_i) = \left(\begin{matrix} [1 - (x_i{}^2 + y_i{}^2)]x_i - \omega_i y_i \\ [1 - (x_i{}^2 + y_i{}^2)]y_i + \omega_i x_i \end{matrix} \right), \qquad (9)$$

where $\mathbf{x}_i \in \mathbb{R}^2$ and $\omega = \omega_i = 3$ is the (identical) intrinsic frequency of each node. Here, the intrinsic instantaneous phase is calculated by $\theta_i = \tan^{-1}(\frac{y_i}{x_i})$. In the latter parts, the upper and lower layers are denoted as layer 1 and layer 2, respectively.

A. Functional relation between η and the amplitude of SL oscillators for interlayer antisynchronization along with intralayer synchronization

First, we consider a set of SL oscillators placed at each node of a multiplex network. Due to our specific choices of G and H, the dynamical evolution of the kth SL oscillator in terms of $z_{\alpha,k} \in \mathbb{C}$ in layer $\alpha (= 1, 2)$ can be written as

$$\dot{z}_{1,k} = (1 - |z_{1,k}|^2)z_{1,k} + i\omega z_{1,k} + \epsilon \sum_{j=1}^{N} \mathscr{A}_{kj}^{[1]}(z_{1,j} - z_{1,k})$$
$$+ \eta(z_{2,k} - z_{1,k}),$$
$$\dot{z}_{2,k} = (1 - |z_{2,k}|^2)z_{2,k} + i\omega z_{2,k} + \epsilon \sum_{j=1}^{N} \mathscr{A}_{kj}^{[2]}(z_{2,j} - z_{2,k})$$
$$+ \eta(z_{1,k} - z_{2,k}). \qquad (10)$$

Let us transform this set of differential equations into polar coordinates using the transformation $z_{\alpha,k} = r_{\alpha,k}e^{i\theta_{\alpha,k}}, \alpha = 1, 2$ and $k = 1, 2, \dots, N$. Under this transformation, the phase equations are given by

$$\dot{\theta}_{1,k} = \omega + \epsilon \sum_{j=1}^{N} \mathscr{A}_{kj}^{[1]} \frac{r_{1,j}}{r_{1,k}} \sin(\theta_{1,j} - \theta_{1,k})$$
$$+ \eta \frac{r_{2,k}}{r_{1,k}} \sin(\theta_{2,k} - \theta_{1,k}),$$
$$\dot{\theta}_{2,k} = \omega + \epsilon \sum_{j=1}^{N} \mathscr{A}_{kj}^{[2]} \frac{r_{2,j}}{r_{2,k}} \sin(\theta_{2,j} - \theta_{2,k})$$
$$+ \eta \frac{r_{1,k}}{r_{2,k}} \sin(\theta_{1,k} - \theta_{2,k}). \qquad (11)$$

Now, when intralayer phase synchronization occurs, we have $\theta_{1,1} = \theta_{1,2} = \cdots = \theta_{1,N}$ and $\theta_{2,1} = \theta_{2,2} = \cdots = \theta_{2,N}$. Therefore, Eq. (11), in terms of two generic nodes j and l, reduces to

$$\frac{d(\theta_{1,j} - \theta_{1,l})}{dt} = \eta \left(\frac{r_{2,j}}{r_{1,j}} - \frac{r_{2,l}}{r_{1,l}} \right) \sin(\theta_{2,j} - \theta_{1,j}),$$
$$\frac{d(\theta_{2,j} - \theta_{2,l})}{dt} = \eta \left(\frac{r_{1,j}}{r_{2,j}} - \frac{r_{1,l}}{r_{2,l}} \right) \sin(\theta_{1,j} - \theta_{2,j}). \qquad (12)$$

Equation (12) confirms the existence of global synchronous solution $\theta_{1,1} = \theta_{1,2} = \cdots = \theta_{1,N} = \theta_{2,1} = \theta_{2,2} = \cdots = \theta_{2,N}$ of the multiplex.

Next, we derive the functional relation between the interlayer coupling strength η and the amplitude of the oscillators $r_{\alpha,k}$ satisfying interlayer antisynchronization state as well as intralayer synchronization. Equations describing the evolution of the amplitude are

$$\dot{r}_{1,k} = (1 - r_{1,k}{}^2)r_{1,k} + \epsilon \sum_{j=1}^{N} \mathscr{A}_{kj}^{[1]}(r_{1,j}\cos(\theta_{1,j} - \theta_{1,k}) - r_{1,k})$$
$$+ \eta(r_{2,k}\cos(\theta_{2,k} - \theta_{1,k}) - r_{1,k}),$$
$$\dot{r}_{2,k} = (1 - r_{2,k}{}^2)r_{2,k} + \epsilon \sum_{j=1}^{N} \mathscr{A}_{kj}^{[2]}(r_{2,j}\cos(\theta_{2,j} - \theta_{2,k}) - r_{2,k})$$
$$+ \eta(r_{1,k}\cos(\theta_{1,k} - \theta_{2,k}) - r_{2,k}). \qquad (13)$$

The complete intralayer synchronization manifolds for each of the two layers yield $r_{1,j} = r_1$ and $r_{2,j} = r_2$ for all $j = 1, 2, \dots, N$ along with $\theta_{1,1} = \theta_{1,2} = \cdots = \theta_{1,N}$ and $\theta_{2,1} = \theta_{2,2} = \cdots = \theta_{2,N}$. So, on the intralayer synchronization manifold, Eq. (13) reduces to

$$\dot{r}_1 = (1 - r_1{}^2)r_1 + \eta(r_2\cos(\theta_{2,k} - \theta_{1,k}) - r_1),$$
$$\dot{r}_2 = (1 - r_2{}^2)r_2 + \eta(r_1\cos(\theta_{1,k} - \theta_{2,k}) - r_2). \qquad (14)$$

For intralayer synchronization together with interlayer antisynchronous solution, we have that $r_1 = r_2$ with $|\theta_{1,k} - \theta_{2,k}| = \pi$, for all $k = 1, 2, \dots, N$. Hence, Eq. (14) can be transformed into

$$\dot{r}_1 = (1 - r_1{}^2)r_1 - 2\eta r_1. \qquad (15)$$

The first-order nonlinear ordinary differential equation (15) leads to

$$(r_1)^2 = \frac{1 - 2\eta}{1 - e^{2(2\eta-1)(t+c_1)}}, \tag{16}$$

where c_1 is a constant depending on the initial conditions. Note that Eq. (16) is undefined for $\eta = \frac{1}{2}$. So, the functional relation between r_1 and η is

$$r_1 = \begin{cases} \frac{\sqrt{1-2\eta}}{\sqrt{1-e^{2(2\eta-1)(t+c_1)}}}, & \eta < \frac{1}{2} \\ \frac{\sqrt{2\eta-1}}{\sqrt{e^{2(2\eta-1)(t+c_1)}-1}}, & \eta > \frac{1}{2}. \end{cases}$$

Equation (15) possesses two stationary points $r_1 = 0$ and $r_1 = \sqrt{1 - 2\eta}$. We will not consider the stationary point $r_1 = 0$ since in Eq. (11) we have assumed $r_{1,k} \neq 0$ and $r_{2,k} \neq 0$. Also, physically $r_1 = 0$ signifies the amplitude death state in both layers, which is a contradiction to the desired assumption of the interlayer antisynchronization in both layers. The other stationary point $r_1 = \sqrt{1 - 2\eta}$ is stable for $\eta < 0.5$.

B. Illustration through bipartite networks

1. Interlayer antisynchronization accompanying intralayer synchronization

A schematic picture of the considered multiplex network is given in Fig. 1(a). For simplicity, we consider the same bipartite network (a four-node ring) in both layers. Initially, all the interlinks (red dashed lines) are repulsive (negative), whereas all the intralinks are positive (attractive). Under this setup, for an intralayer coupling strength $\epsilon = 0.007$, all the four trajectories of a single layer converge to a single attractor. Both layers exhibit intralayer synchronization [see Figs. 1(c) and 1(d)]. However, when the interlinks are repulsive (coupling strength $\eta = -0.1$), antisynchronization between both layers arises [see Fig. 1(b)]. Note that, in this particular example, networks within each layer are identical.

To show a more general example, we now consider layers of different structure. Specifically, we construct a bilayer bipartite multiplex in which layer 1 consists a ring of six nodes and layer 2 has an open chain of six nodes (Fig. 2).

All nodes in both layers are attractively coupled with $\epsilon = 0.01$. Only the six interlinks are negatively coupled with coupling strength $\eta < 0$. With suitable values of η, replica nodes maintain *interlayer antisynchronization state*. In Fig. 2(c), time series show, for $\epsilon = 0.01$ and $\eta = -3.0$, that all trajectories within the same layer collapse into a single attractor, which proves the emergence of *intralayer synchronization*. At the same time, replica nodes exhibit *interlayer antisynchronization*. To better understand phase relations inside the multiplex network, we calculated F_{Layer1}, F_{Layer2}, F_{Replica}, and F as a function of $\eta \in [-1.1, 1.0]$ with fixed $\epsilon = 0.01$. As we can see in Fig. 2(b), F_{Layer1} and F_{Layer2} are exactly 2 even for negative η. This fact indicates the existence of intralayer (in-phase) synchronization at both layers under this particular arrangement of negative links. However, F_{Replica} goes to 0 with suitable repulsive coupling strength η and remains at 0 for $\eta < 0$. $F_{\text{Replica}} = 0$ implies *interlayer antiphase synchronization* as well as the onset of *interlayer antisynchronization*. The nonzero values of F_{Layer1} and F_{Layer2} restrict, in turn, F to
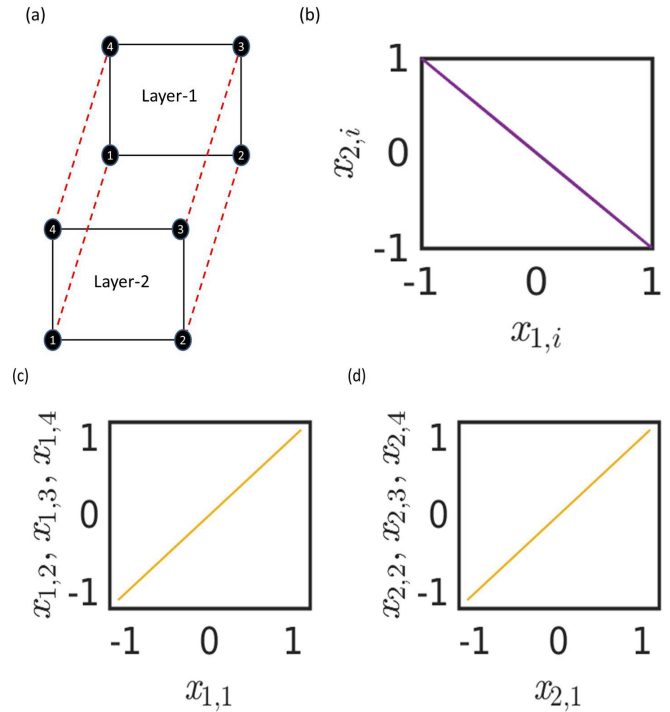

FIG. 1. Intralayer synchronization and interlayer antisynchronization. Two bipartite graphs are multiplexed through repulsive (i.e., negative) coupling. In (a), black solid lines correspond to positive intralinks and red dashed lines represent negative interlinks. Such an arrangement allows intralayer synchrony and interlayer antisynchrony regimes for suitable choices of positive and negative coupling strengths. In (b), (c), and (d), we plot the trajectories of standard Stuart-Landau oscillators, with $\omega = 3.0$, which are placed at each of the nodes of (a). For all plots, $\epsilon = 0.007$ and $\eta = -0.1$. In (b), we can observe how trajectories of nodes belonging to layer 1 ($x_{1,i}$) are antisynchronized with respect to nodes in layer 2 ($x_{2,i}$). At the same time, nodes in layer 1 and layer 2 are synchronized, as shown in (c) and (d), respectively.

a nonzero value, which reflects the absence antiphase states within adjacent nodes in the entire network.

To calculate the value of F theoretically [46], let the phase of each oscillator in one layer be 0 and the other layer's oscillators have a phase π. Using the proposed measure F, the value of $F_{\text{Layer}\alpha}$ will be exactly 2 for all intralinks since all phases in the same layer are identical (i.e., either 0 or π). But, all the interlinks are contributed exactly $F_{\text{Replica}} = 0$ for *interlayer antiphase synchronization state*. Thus, all the 11 intralinks are contributing with $11 \times 2 = 22$ and, thus, $F = \frac{22}{17} \approx 1.29$ since the denominator 17 is the total number of links of the multiplex network. This theoretical value of F perfectly fits with our numerical calculation as shown in Fig. 2(b). Nodes are colored in Fig. 2(a) according to the final phase of each oscillator. As both the layers exhibit intralayer synchronization, all nodes of a particular layer can be colored with a single color. Note that the oscillators situated on the top of replica nodes maintain a phase difference of π. Thus, the two layers can be colored with two distinct colors only.

What happens if we have multiplex networks of larger size? We now construct a bipartite multiplex network of
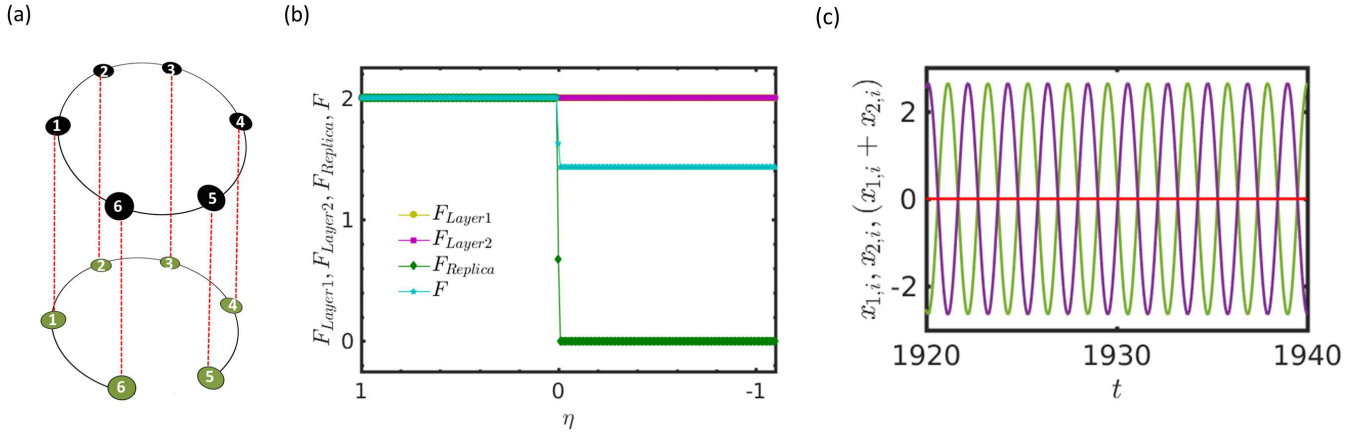
FIG. 2. Multiplex network composed of two layers with different structures. In (a), structure of the two layers. Layer 1 (upper layer) has a ring configuration, while Layer 2 (lower layer) is an open chain. Solid lines correspond to (intralayer) positive links and dashed lines to (interlayer) negative links. We place a Stuart-Landau oscillator at each node. In (b), we show the dependence of F_{Layer1}, F_{Layer2}, $F_{Replica}$, and F as a function of the coupling strength η of the interlayer links. We can observe the transition of $F_{Replica}$ and F when η becomes negative. In (c), example of interlayer antisynchronization with intralayer synchronization, for $\eta = -3.0$. We plot the dynamics of all nodes $x_{1,i}$ (magenta lines), $x_{2,i}$ (green lines), and $x_{1,i} + x_{2,i}$ (red lines) as a function of time t after an initial transient. Note that lines of nodes of the same layer overlap. The amplitude of the oscillators follows the analytical expression $r_1 = \sqrt{1 - 2\eta}$.

size 200, with two connected Erdős-Rényi random networks [65,66] of 100 nodes in each layer. The average degree of each layer is close to 5. The intralayer coupling strength between nodes of layers is fixed to $\epsilon = 0.01$. When the interlinks are only negative (i.e., $\eta < 0$) of suitable strength, then $F_{Replica} = 0$ implying *interlayer antiphase synchronization*. Figure 3(a) shows the variation of F, F_{Layer1}, F_{Layer2}, and $F_{Replica}$ with respect to η. In this case, both layers exhibit intralayer (in-phase) synchronization, as indicated by $F_{Layer1} = 2$ and $F_{Layer2} = 2$. In fact, they are in *intralayer synchronization* and the oscillators on the top of replica nodes exhibits *interlayer antisynchronization* [see Fig. 3(b)]. To calculate value of F for $\eta < 0$, the phase of each oscillator of layer 1 is set to 0 and phases of layer-2 oscillators are set to π, without loss of any generality. Then, the definition of F leads to $F = \frac{478 \times 2}{578} \approx 1.65$. Here, the numerator reflects the value of the 478 intralinks and the denominator indicates the total number of links (578) of the whole multiplex. This theoretical value fits with the numerically calculated value of F, which is shown in Fig. 3(a). Note that this repulsive configuration cannot lead to *antiphase synchronization* between all pairs of adjacent nodes in the network (i.e., $F = 0$). In the next section, we will show how to achieve *antiphase synchronization* in a bipartite multiplex networks.

In Fig. 4, we plot the amplitude of the oscillators r_1 with respect to η varied from 0 to -20 with step size $\Delta_\eta = -0.1$. For the numerical simulation, r_1 is accumulated for 10 independent numerical realizations averaged over a long time interval after sufficient initial transient. Numerical results fit perfectly with our analytical solution $r_1 = \sqrt{1 - 2\eta}$ for $\eta \leqslant 0$. This relation ensures the attractor expansion of SL oscillators given in Eq. (9) during interlayer antisynchronous solution together with the intralayer synchronization for $\eta < 0$. We have shown later using master stability function that interlayer antisynchronization is possible beyond a negative η. We ignore here the impact of positive η as the main motivation of our work

related to antisynchronization (antiphase synchronization) in the multiplex network.

Finally, note that our derived analytical relation $r_1 = \sqrt{1 - 2\eta}$ is independent of N. In Fig. 4, we plot the relation for the multiplex network consisting of 8 nodes given in Fig. 1, we obtain exactly the same results for the multiplex of 200 nodes used in Fig. 3. We can observe how the radial distance r_1 is monotonically increasing with respect to the interlayer coupling strength $\eta < 0$. As the trajectories in each layer maintain intralayer synchronization, we plot the radial distance r_1 of a single trajectory only.

2. Antiphase synchronization *in adjacent nodes*

Now, we investigate how to establish antiphase synchrony in the whole multiplex network. Specifically, we are interested in determining how many repulsive links are sufficient to achieve antiphase synchronization. To gain such antiphase states between adjacent nodes, we uncover that we have to replace interlinks as well as the links of a spanning tree of any one of the connected layer by repulsive strength $\eta < 0$. It is always possible to find a spanning tree of any one of the layer since every connected graph possesses at least one spanning tree. For the multiplex network given in Fig. 1(a), we choose layer 2 without any loss of generality. Thus, the original model given in Eq. (1) changes to

$$\dot{\mathbf{x}}_{1,i} = f(\mathbf{x}_{1,i}) + \epsilon \sum_{j=1}^{N} \mathscr{A}_{ij}^{[1]} G[\mathbf{x}_{1,j}, \mathbf{x}_{1,i}] + \eta H[\mathbf{x}_{2,i}, \mathbf{x}_{1,i}],$$

$$\dot{\mathbf{x}}_{2,i} = f(\mathbf{x}_{2,i}) + \epsilon \sum_{j=1}^{N} \mathscr{D}_{ij}^{[2]} G[\mathbf{x}_{2,j}, \mathbf{x}_{2,i}]$$

$$+ \eta \sum_{j=1}^{N} \mathscr{E}_{ij}^{[2]} G[\mathbf{x}_{2,j}, \mathbf{x}_{2,i}] + \eta H[\mathbf{x}_{1,i}, \mathbf{x}_{2,i}]. \quad (17)$$
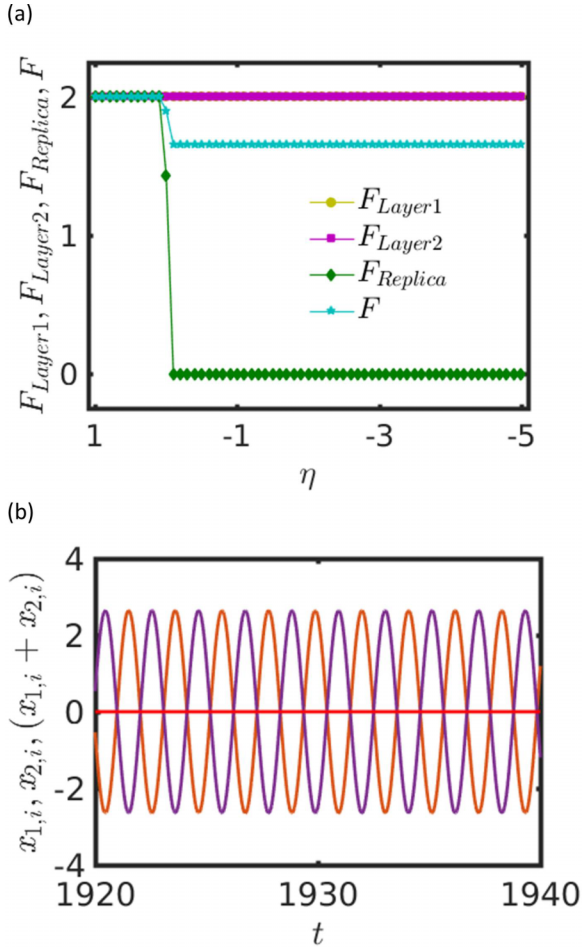
(a)

(b)

FIG. 3. Dynamics of a multiplex network composed of 200 nodes. In this example, the two layers contain distinct bipartite graphs of 100 nodes with an average degree of 5. The intralayer coupling strengths are set to $\epsilon = 0.01$ and the $N = 100$ interlinks have a strength of η. In (a), η is varying uniformly from 1.0 to -5.0 with step of $\Delta_\eta = -0.1$. We can see that $F_{\text{Layer1}} = F_{\text{Layer2}} = 2$ reveals the existence of intralayer in-phase synchronization. At the same time, we observe how as η becomes ≈ -0.1, interlayer antiphase synchronization arises, as indicated by $F_{\text{Replica}} = 0$. In (b), we plot the dynamics of all oscillators, separated by layers: $x_{1,i}$ (magenta lines), $x_{2,i}$ (green lines), and $x_{1,i} + x_{2,i}$ (red lines). The fact that $x_{1,i} + x_{2,i} = 0$ proves the existence of interlayer antisynchronization. In this realization, $\eta = -3.0$ and $\epsilon = 0.01$.

Here, the intralayer adjacency matrix $\mathscr{A}_{ij}^{[2]} = \mathscr{D}_{ij}^{[2]} + \mathscr{E}_{ij}^{[2]}$ of layer 2 is decomposed into two parts $\mathscr{D}_{ij}^{[2]}$ and $\mathscr{E}_{ij}^{[2]}$. Through one subgraph $\mathscr{D}_{ij}^{[2]}$, positive coupling strength ϵ is considered and the complementary subgraph $\mathscr{E}_{ij}^{[2]}$ contains negative couplings ($\eta < 0$) between the oscillators. Along with this, the interlinks are also considered to have a negative weight η, as in earlier sections. The particular structure of the layer 2 in Fig. 1(a) is a four-node ring, which has exactly $\binom{4}{3} = 4$ distinct spanning trees. A spanning tree consisting on links $1 - 2$, $2 - 3$, and $3 - 4$ [red dashed links in Fig. 5(a)] is considered. Along the branches of this spanning tree, the coupling strength is set to $\eta = -0.1$ (same as the interlayer coupling), keeping the intralayer coupling as $\epsilon = 0.007$. For
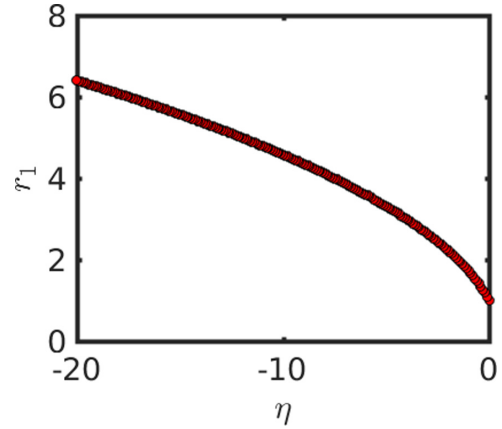

FIG. 4. Relation between η and r_1 of Stuart-Landau oscillators. In the numerical simulations, η is varied between $[-20, 0]$ with a fixed uniform step of $\Delta_\eta = -0.1$. The numerical curve fits perfectly with our analytical findings. Here, we have used the multiplex network shown in Fig. 1 with $\epsilon = 0.01$. The same results (not shown here) are obtained for the multiplex network of 200 nodes shown in Fig. 3.

these repulsive edges, nodes show neighborwise antiphase synchrony, as we can see in Figs. 5(b)–5(g). Thus, just by introducing the suitable repulsive strength to the intralinks of the spanning tree of a unique layer (layer 2 in this example), we can establish antiphase synchronization in the whole network, if the multiplex network is bipartite.

In this way, we choose a spanning tree of the layer 2 belonging to the multiplex network shown in Fig. 2(a). Next, the coupling strength of all links of this spanning tree is replaced by a negative value η (instead of $\epsilon > 0$). A schematic presentation is given in Fig. 6(a). Under this arrangement, we set $\epsilon = 0.01$ and modify the value of η from 1.0 to -1.1, with a fixed step of -0.01. For these parameters, we calculate F_{Layer1}, F_{Layer2}, F_{Replica}, and F, whose values are shown in Figure 6(b). We can observe that at $\eta \approx -0.1$, F diminishes to 0, together with F_{Layer1}, F_{Layer2}, F_{Replica}. Thus, the spanning tree of a single layer is sufficient to produce antiphase synchrony in the whole multiplex network. We color the nodes of Fig. 6(a) according to their final phases. A minimum of two colors is required to produce a proper coloring of the multiplex network since each adjacent oscillator displays a phase difference of π.

We can see that the number of repulsive links $L_{\text{Repulsive}}$ in the whole multiplex in such arrangement is $L_{\text{Repulsive}} = 11$, where the spanning tree of layer 2 has 5 links and there are 6 repulsive interlinks. Now, we inspect numerically whether we need exactly 11 repulsive links to attain antiphase synchronization of the whole multiplex, or if it would be possible with a lower number of repulsive links. Figure 6(c) shows the role of $L_{\text{Repulsive}}$ on the measures F_{Layer1}, F_{Layer2}, F_{Replica}, and F. When $L_{\text{Repulsive}} = 6$, i.e., only interlinks are negatively coupled, then only $F_{\text{Replica}} = 0$ with F_{Layer1}, F_{Layer2} and F having values greater than 0. This result is consistent with the Figs. 2(b) and 2(c). Now, the number of repulsive links is increased by introducing the repulsive strength $\eta = -3.0$ through the links of the spanning tree. Figure 6(c) shows that increments of $L_{\text{Repulsive}}$ decrease the
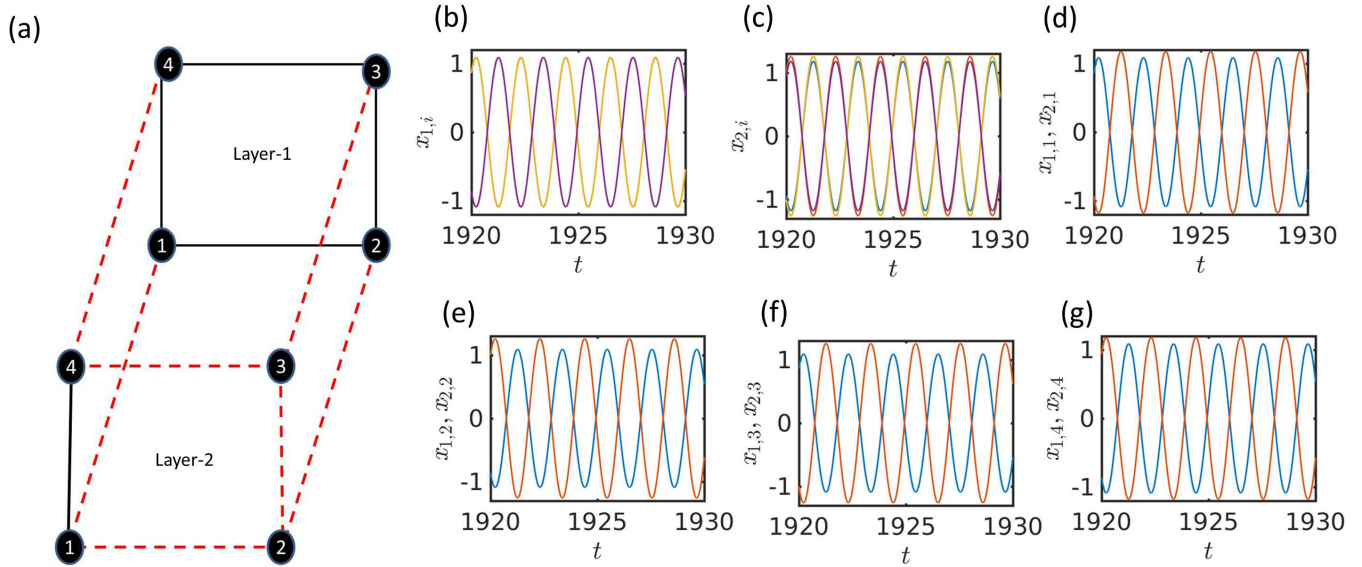
FIG. 5. Introducing additional $(N-1)$ repulsive links through a spanning tree. In (a), for the multiplex network of Fig. 1, we select a spanning tree in layer 2. Together with the interlinks, the intralayer links of the spanning tree are set to have a coupling strength of $\eta < 0$. All negative links are indicated by dashed lines. The other intralinks of layer 1 are positively coupled with coupling strength $\epsilon > 0$ and the remaining links of layer 2 are also coupled with $\epsilon > 0$. In this way, positive links are plotted in black solid lines. In (b)–(g), we show some examples of antiphase synchronization. All nodes of all layers exhibit neighborwise antiphase synchrony. For these numerical simulations, $\epsilon = 0.007$ and $\eta = -0.1$.

values of F, F_{Layer1}, F_{Layer2}, which become all zero only when $L_{\text{Repulsive}} = 11$, i.e., until all the links of the spanning tree are negative. These results agree with the theoretical results of Sec. III D.

Next, we repeat the same procedure with the multiplex network of 200 nodes described in Fig. 3. Again, we find a spanning tree of layer 2 and replace the coupling strength

of the links of the spanning tree by $\eta < 0$ instead of $\epsilon > 0$. For a suitable choice of η, the system achieves antiphase synchronization, as revealed by $F = 0$, $F_{\text{Layer1}} = 0$, and $F_{\text{Layer2}} = 0$ [see Fig. 7(a)]. In Fig. 7(b), we show the effect the number of repulsive links, $L_{\text{Repulsive}}$ on the measures F_{Layer1}, F_{Layer2}, F_{Replica}, and F. Initially, $N = 100$ interlinks are coupled through $\eta = -3.0$. Then, one by one, links of
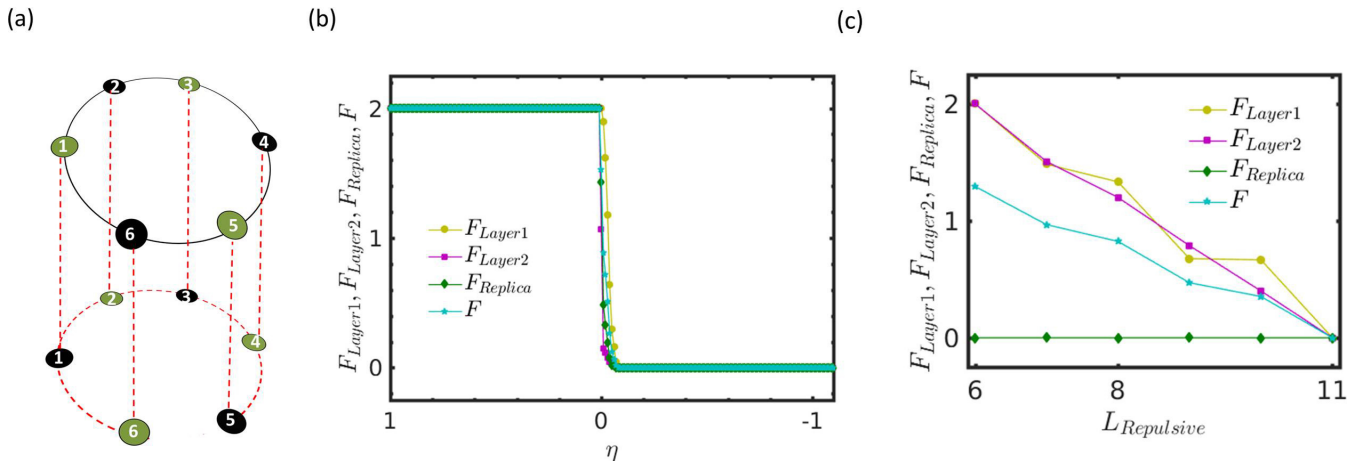

FIG. 6. Selecting a repulsive spanning tree when layers have different structures. In (a), we select a spanning tree in layer 2 and set their couplings to be $\eta < 0$, just as the coupling strength of the interlinks. Red dashed lines are negative links and black links are positive links. Here, $\eta = -0.1$ and ϵ is fixed at 0.01 just like Fig. 2(a). All nodes are colored according to their phases. In (b), we show the effect of the negative coupling: η is varied, with step of $\Delta_\eta = -0.01$, from 1.0 to -1.1. Note that for $\eta < 0$, the whole network exhibits antiphase synchronization as indicated by $F = 0$. Layerwise antiphase and interlayer antiphase synchronization are both indicated by $F_{\text{Layer1}} = 0$, $F_{\text{Layer2}} = 0$, and $F_{\text{Replica}} = 0$. In (c), we show the effect of increasing the number of repulsive links $L_{\text{Repulsive}}$ in the spanning tree. Initially, only interlinks are repulsive, i.e., $L_{\text{Repulsive}} = N = 6$. At this point, $F_{\text{Replica}} = 0$, $F_{\text{Layer1}} = F_{\text{Layer2}} = 2$. These values imply interlayer antiphase synchronization along with layerwise in-phase synchrony. Increasing $L_{\text{Repulsive}}$ up to $(2N-1) = 11$, by introducing the negative links through the spanning tree of layer 2, we achieve antiphase synchronization as indicated by $F = 0$. In these numerical simulations, $\eta = -3.0$ and $\epsilon = 0.01$.
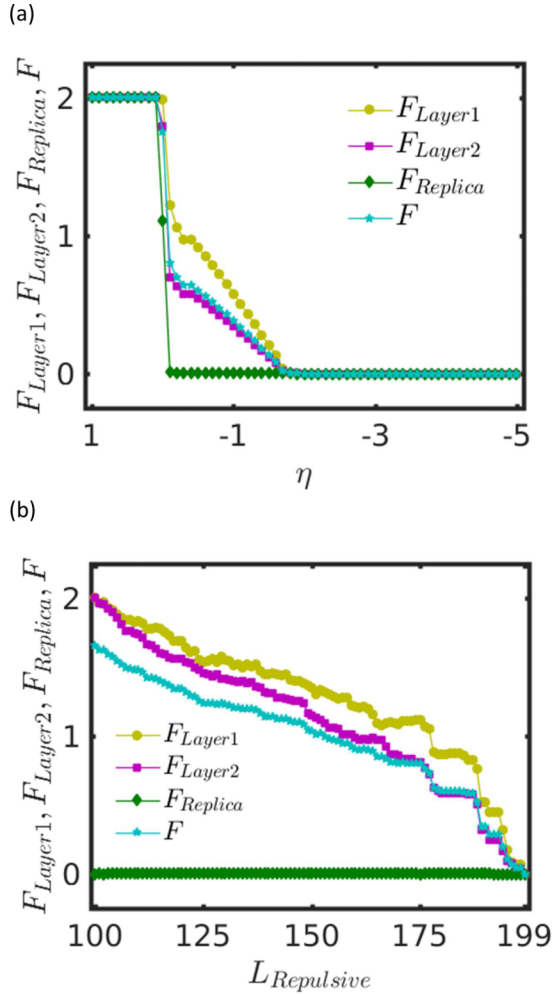
(a)

(b)

FIG. 7. Repulsive spanning tree in a multiplex network of 200 nodes. We identify a spanning tree in layer 2 of the multiplex network of Fig. 3 (containing 100 nodes per layer). Links in the spanning tree are set to have a coupling strength of η, while the coupling of the rest of the intralayer links is $\epsilon = 0.01$. In (a), we can observe how the negative links of the spanning tree help to reach antiphase synchronization ($F = 0$) in the whole multiplex network. At a suitable choice of $\eta < 0$, F_{Layer1}, F_{Layer2}, and F all collapse into 0. In (b), we investigate the effect of the number of repulsive links $L_{\text{Repulsive}}$ in the spanning tree. Initially, only the 100 interlinks are negative. Then, additional $(N - 1) = 99$ repulsive links are introduced through the spanning tree of layer 2. For the numerical simulations, $\eta = -3.0$ and $\epsilon = 0.01$.

the spanning tree of layer 2 are set to have a coupling strength $\eta = -3.0$ instead of $\epsilon > 0$. As a consequence, the gradual decrement of F_{Layer1}, F_{Layer2}, and F to zero shows the emergence of antiphase synchronization for the whole multiplex.

Until now, all results referred only to bilayer multiplex networks. To show that this methodology can be applied to multiplex networks with more layers, we consider a bipartite multiplex network with three different connected layers in the chain form. In the next example, each layer contains three different bipartite Erdős-Rényi random graphs [65,66] of 100 nodes. The average degree of the multiplex network
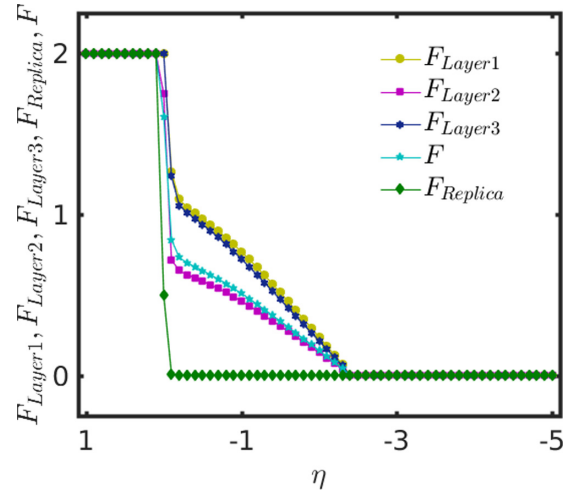
FIG. 8. Negative spanning tree in a bipartite multiplex network with three layers, each one having $N = 100$ nodes. In this case, the multiplex network is composed of three layers. A spanning tree of layer 2 is chosen and the $(N - 1) = 99$ links of the spanning tree together with the $2 \times N = 200$ interlinks are set to have a coupling strength η, which is varied from 1.0 to -5.0 with a step of $\Delta_\eta = -0.1$. The three layers have the identical intracoupling strength $\epsilon = 0.01$. For positive η, the system has in-phase synchrony, indicated by $F = 2$, $F_{\text{Layer1}} = 2$, $F_{\text{Layer2}} = 2$, $F_{\text{Layer3}} = 2$, and $F_{\text{Replica}} = 2$. As η becomes negative with sufficient strength, F_{Replica} diminishes to 0 and, then, interlayer antiphase synchronization arises. For more negative values of η, F along with F_{Layer1}, F_{Layer2}, F_{Layer3}, and F_{Replica} collapse to 0 implying antiphase synchronization.

is ($\approx$) 7. Figure 8 shows how F_{Layer1}, F_{Layer2}, F_{Layer3}, F_{Replica}, and F depend on the value of η. The definition of F_{Replica} is slightly modified by adding the information of interlinks between layer 2 and layer 3, i.e.,

$$F_{\text{Replica}} = \left\langle \frac{1}{2N} \sum_{i=1}^{N} [2 + \cos(\theta_{1,i} - \theta_{2,i}) + \cos(\theta_{3,i} - \theta_{2,i})] \right\rangle_t. \tag{18}$$

We divide by $2N$ as there are $2N$ interlinks contributing in this measure.

Without loss of generality, we choose a particular spanning tree of layer 2 and the $(N - 1) = 99$ links of belonging to spanning tree together with the $2N = 200$ interlinks are set to have a coupling strength $\eta < 0$. The intracoupling strengths are fixed at $\epsilon = 0.01$. Just by controlling a subgraph (i.e., the spanning tree) of layer 2, we are able to achieve antiphase synchronization of the whole multiplex network. Negative values of η make go to $F_{\text{Replica}} = 0$ and induce a reduction of the values of F, F_{Layer1}, F_{Layer2}, and F_{Layer3}, becoming all zero when η is decreased enough. This implies the appearance of interlayer antiphase synchronization just like the case of bilayer multiplex networks. Actually, the $(N - 1) + 2N = (3N - 1)$ links coupled via $\eta < 0$ form a spanning tree for the whole three-layer bipartite multiplex network.
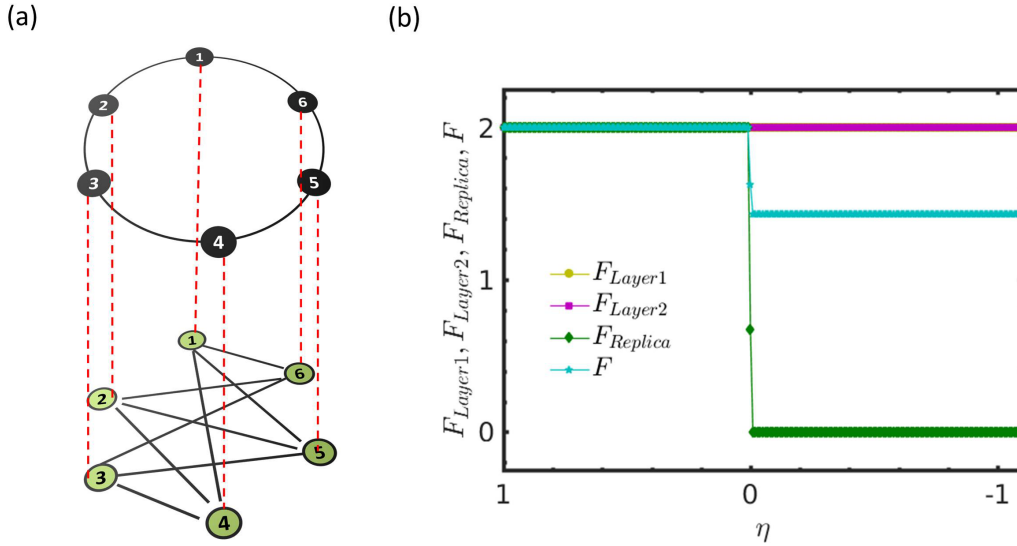
FIG. 9. Antisynchronization in nonbipartite multiplex networks. In (a), we show an example of a nonbipartite multilayer network. Layer 1 contains a ring of six nodes and layer 2 is a bipartite regular network of average degree 3. Despite both layers contain bipartite networks, the multiplex network is not bipartite since it contains odd cycles. The colors of the vertices represent the phases of the oscillators. Interlinks have a negative coupling strength $\eta = -0.1$, while intralinks are set to $\epsilon = 0.01$. In (b), dependence of the phase measures on η. $F_{\text{Layer1}} = 2$ and $F_{\text{Layer2}} = 2$ indicate the existence of intralayer in-phase synchronization. When $F_{\text{Replica}} = 0$ (when $\eta < 0$) interlayer antiphase synchronization is achieved. However, intralayer in-phase synchrony hinders the decrement of F to zero. In these simulations, the interlinks are coupled with η while the intralayer coupling strength is $\epsilon = 0.01$.

C. Result for small nonbipartite multiplex network

We discussed in Sec. III F that if a multiplex network is bipartite, then the connected networks of each layer must be bipartite. However, the converse may not be true. To prove this argument, we consider the multiplex network of 12 nodes shown in Fig. 9(a). Here, layer 1 consists of a ring of six nodes and layer 2 consists of a bipartite regular graph of degree 3. So, clearly the two intralayer networks are bipartite, but the multiplex network is not bipartite due to existence of odd cycles. One such odd cycle is formed by including nodes 4 and 5 of layer 1 and nodes 2, 4, and 5 of layer 2. As per our theoretical discussion in Sec. III E and for our chosen coupling functions, interlayer antisynchronization along with intralayer synchronization is still possible in this multiplex network. In Fig. 9(b), we show the variation of F, F_{Layer1}, F_{Layer2}, and F_{Replica} with respect to η (with $\epsilon = 0.01$), when only the interlinks have a coupling strength η. We can observe how, for a suitable strength of $\eta < 0$, $F_{\text{Replica}} = 0$ indicates the existence of the interlayer antiphase synchronization. $F_{\text{Layer1}} = 2 = F_{\text{Layer2}}$ indicates the in-phase synchrony of both layers. The nonzero values of F_{Layer1} and F_{Layer2} restrict the decrement of F to zero. Again, applying the definition of F, we find $F = \frac{2 \times 15}{21} \approx 1.43$, where the number of links of the whole multiplex network is 21 and the number of intralinks is 15. This theoretical value of F agrees with the numerical findings shown Fig. 9(b).

In Fig. 10, we plot the dynamics of $x_{1,i}$, $x_{2,i}$, and $x_{1,i} + x_{2,i}$ with respect to time t. The interlinks are repulsive with a coupling strength of $\eta = -3.0$, while the intralayer coupling strength is set to $\epsilon = 0.01$. Since our proposed measures do not contain any information about the am-

plitude of the variables, Fig. 10 shows the existence of interlayer antisynchronization since $x_{1,i} + x_{2,i} = 0$. Also, intralayer synchronization arises since all trajectories within a layer converge to a single one. Furthermore, note that amplitudes of the SL oscillators maintain the analytically expression found in Sec. IV A ($r_1 = \sqrt{1 - 2\eta}$).

Next, the links of a spanning tree of layer 2 are set to have a coupling strength of $\eta < 0$ [see Fig. 11(a)]. We plot in Fig. 11(b) the values of F, F_{Layer1}, F_{Layer2}, and F_{Replica} for $\eta \in [-1.1, 1]$. In this case, F_{Layer2} decreases to zero indicating antiphase synchrony between neighbors of layer 2, but F lies between (0, 2). Actually, both layers contain bipartite graphs and, thus, it is possible to define two-colorable graphs as shown by the colors of the nodes in Fig. 11(a). However,
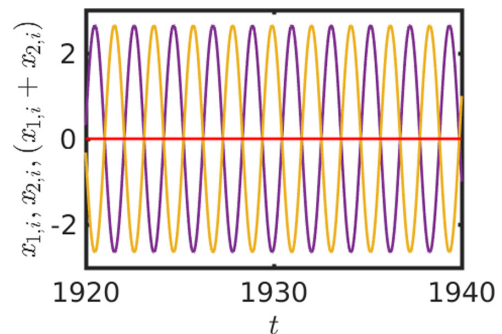

FIG. 10. Intralayer synchronization and interlayer antisynchronization for the multiplex network of Fig. 9. Here, $\epsilon = 0.01$ (intralink coupling) and $\eta = -3.0$ (interlink coupling). The amplitude of the oscillators still maintains the analytical rule $r_1 = \sqrt{1 - 2\eta}$.
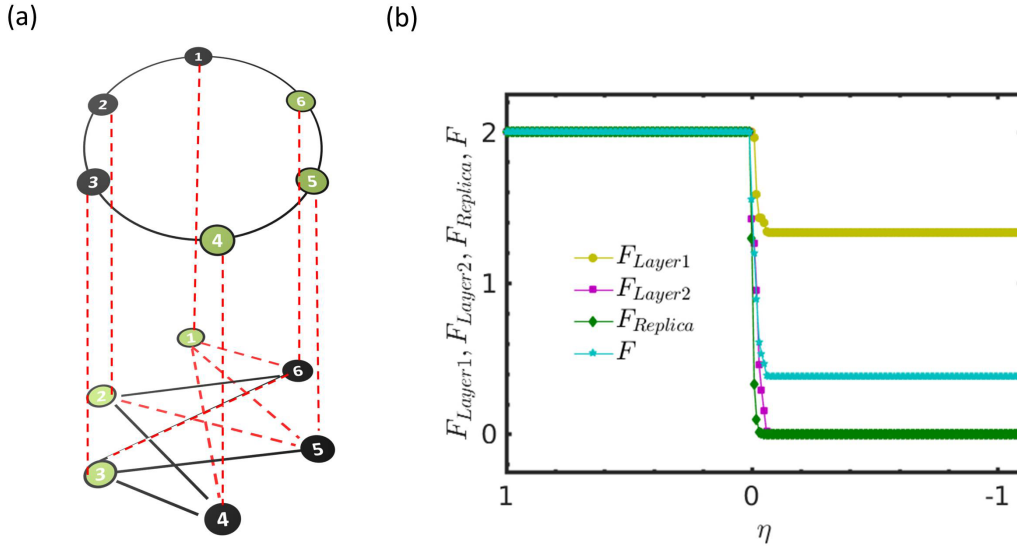
FIG. 11. Using a negative spanning tree in a nonbipartite multilayer network. In (a), we identify a spanning tree in layer 2 of the multiplex network of Fig. 9 and set its links to a coupling strength of $\eta = -0.1$. These negative links help to attain antiphase synchronization in layer 2, however, the odd cycles in the multiplex hinder antiphase synchrony. The color of each node indicates the phase of the oscillator. In (b), we analyze the evolution of the phase metrics as a function of the coupling η (of the interlinks and the links of the spanning tree), for the network shown in (a). $F_{\text{Layer2}} = 0$ indicates the existence of antiphase synchronization in layer 2, but the odd cycles of the multiplex network do not allow the reduction of F to zero. In fact, layer 1 has two distinct phases, but $F_{\text{Layer1}} \neq 0$. However, we still can achieve interlayer antiphase synchronization, as indicated by $F_{\text{Replica}} = 0$.

interlinks create odd cycles and, hence, the multiplex network is a nonbipartite graph. This fact prevents F diminishing to zero. This result is consistent with our analytical findings indicating that antiphase synchronization is only possible *if and only if* the underlying network is bipartite in nature. Nodes of layer 2 separate into two disjoint groups $U_2 = \{1, 2, 3\}$ (shown in olive green) and $V_2 = \{4, 5, 6\}$ (shown in black). Layer 2 is in antiphase synchronization since $F_{\text{Layer2}} = 0$, and $F_{\text{Replica}} = 0$ implies interlayer antiphase synchronization. As a consequence, the graph coloring for layer 1 is $U_1 = \{1, 2, 3\}$ (black) and $V_1 = \{4, 5, 6\}$ (olive green). Without any loss of generality, we assign phase 0 to the set U_2 and phase π of the set V_2. Thus, $F_{\text{Replica}} = 0$ implies that phases of the set U_1 are π and the phases of set V_1 are 0. Using the formula for F_{Layer1}, one can find, analytically, that $F_{\text{Layer1}} = \frac{8}{6}$, which fits with the value of F_{Layer1} obtained numerically [see Fig. 11(b)].

V. CONCLUSION

We investigated the synchronization of multiplex networks of identical oscillators with positive and negative links. Most of the earlier existing investigations on multilayer networks have been concentrated only on positive coupling, which helps to the emergence of in-phase synchronization. On the other hand, negative coupling, analogous to antiferromagnetic interaction, disturbs the in-phase synchronization manifold and drives the oscillator out of phase. The coexistence of both types of interactions affects the collective dynamics of the system and displays rich dynamical phenomenon. In this study, we showed that adequately tuning the positive coupling between oscillators, it is possible to reach intralayer synchronization of multiplex networks. However, when the strength of the interlinks (between layers) becomes negative,

interlayer antisynchronization can be achieved, where both layers oscillate with exactly the same amplitude but a phase difference of π. The invariance of intralayer synchronization manifold is guaranteed when the undirected networks contained in each layer are regular, or when the intralayer coupling function disappears at the intralayer synchronization manifold. We analytically derived the necessary condition for the existence of interlayer antisynchronization together with intralayer synchronization. When Stuart-Landau oscillators are implemented in the multiplex network, the conversion from Cartesian coordinates to polar coordinates allows us to analytically calculate the radius of each oscillator, which agrees with our numerical simulations for negative interlayer coupling strength.

We also investigated an efficient way of achieving antiphase synchronization in multiplex networks. Instead of introducing repulsive links through the whole multiplex network, we select any spanning tree of one of the connected layers of the multiplex. Introducing negative couplings in the links of the spanning tree, antiphase synchronization can be obtained without perturbing the rest of the network. The existence of at least one spanning tree in a connected network guarantees the occurrence of antiphase patterns in bipartite multiplex networks when the coupling strengths are adequately adjusted. Our analytical findings were also tested with numerical simulations of different multiplex networks. The use of spanning trees is simple and cost effective compared to the introduction of negative links in the whole population. Furthermore, this controlling scheme may have some potential applications, particularly in those cases where it is demanding to choose few links out of a large number.

Finally, our findings may be helpful in order to understand the emergent different dynamical phenomena in

those complex systems that combine excitatory and inhibitory couplings. For example, a natural instance may be neuroscience since the brain has all requisites existing in our model. First, brain functioning relies on the existence of combined excitatory and inhibitory neurons [67,68]. Second, antiphase synchronization has been reported in cortical neuronal networks [43]. Third, multilayer brain networks have been suggested to be behind healthy and impaired brain functioning, being one of the most promising tools to understand the complex topological behavior of brain dynamics [69,70]. Beyond neuroscience, our results could be of interest to investigate the dynamical consequences of mixed attractive-repulsive interaction in biological systems, ecological systems, and social systems.

APPENDIX: STABILITY OF INTERLAYER ANTISYNCHRONIZATION STATE

We investigate the stability of the interlayer antisynchronization in multiplex network which is defined by two types of connections: (i) diffusive intralayer connections in each layer and (ii) repulsive interlayer connections between layers. The evolution of the oscillators contained in a bilayer network can be written as

$$\dot{\mathbf{x}}_{1,i} = f(\mathbf{x}_{1,i}) - \epsilon \sum_{j=1}^{N} \mathscr{L}_{ij} G \mathbf{x}_{1,j} + \eta H[\mathbf{x}_{2,i} - \mathbf{x}_{1,i}],$$

$$\dot{\mathbf{x}}_{2,i} = f(\mathbf{x}_{2,i}) - \epsilon \sum_{j=1}^{N} \mathscr{L}_{ij} G \mathbf{x}_{2,j} + \eta H[\mathbf{x}_{1,i} - \mathbf{x}_{2,i}], \quad \text{(A1)}$$

where i ($i = 1, 2, \ldots, N$) is the oscillator index. As our objective here is to study the interlayer antisynchronization, we consider the vector field f to be identical for each node. Here, $H \in \mathcal{M}_d(\mathbb{R})$ and $G \in \mathcal{M}_d(\mathbb{R})$ are, respectively, the interlayer and intralayer inner coupling matrices. We assume that f is continuously differentiable with respect to its argument. Here, ϵ is the intralayer coupling strength which controls the interaction between the nodes in each layer. The interlayer coupling strength η determines how the interaction will be conveyed between the layers. When η is positive, then the interlayer coupling is attractive, for which the multiplex network exhibits intralayer and interlayer synchronization [31,35]. However, when η is negative, the interlayer coupling is repulsive.

In the αth layer ($\alpha = 1, 2$), the intralayer network configuration is encoded by the $N \times N$ adjacency matrix $\mathscr{B}$ which describes the interconnections between individual oscillators for that layer. Here, $\mathscr{B}_{ij} = 1$ if the ith and the jth nodes of layer α are connected, and zero otherwise. Let, $\mathscr{L}$ be the corresponding zero-row sum Laplacian matrix, defined as $\mathscr{L}_{ij} = -\mathscr{B}_{ij}$ if $i \neq j$ and $\mathscr{L}_{ii} = \sum_{j=1}^{N} \mathscr{B}_{ij}$.

Interlayer antisynchronization is an emerging phenomenon of a multiplex network in which nodes of one layer evolve antisynchronously with its replica nodes of the different layers, irrespective of whether the nodes in the same layer are in any synchrony or not. Mathematically, network (A1) is said to achieve the interlayer antisynchronization state if for all $i = 1, 2, \ldots, N$, $\|\mathbf{x}_{1,i}(t) + \mathbf{x}_{2,i}(t)\| \to 0$ as $t \to \infty$. Then, we can define the corresponding interlayer antisynchronization error as

$$E = \lim_{t_1 \to \infty} \frac{1}{t_1} \int_t^{t+t_1} \sum_{j=1}^{N} \frac{\|\mathbf{x}_{1,i}(\tau) + \mathbf{x}_{2,i}(\tau)\|}{N} \, d\tau. \quad \text{(A2)}$$

E necessarily becomes zero when interlayer antisynchronization arises, and remains nonzero otherwise.

Then, the interlayer antisynchronization subspace can be defined as $\mathcal{S} = \{(\mathbf{x}_{1,1}(t), \mathbf{x}_{1,2}(t), \ldots, \mathbf{x}_{1,N}(t)) \subset \mathbb{R}^{dN} : \mathbf{x}_{1,i}(t) + \mathbf{x}_{2,i}(t) = 0$ for all $i = 1, 2, \ldots, N$ and $t \in \mathbb{R}^+\}$. If this subspace is stable with respect to perturbations in its transverse subspace, then the interlayer antisynchronization state could be achieved at the multiplex network. We now derive the analytical stability condition for the interlayer antisynchronization state in a generic multiplex network (A1) using the master stability function (MSF) approach [71].

For multiplex networks, the MSF has been extended by considering the static [72] and time-varying [31,35] network architectures, allowing to identify the analytical conditions for intralayer and interlayer synchronization.

When interlayer antisynchronization is achieved, we have that

$$\dot{\mathbf{x}}_{1,i} = f(\mathbf{x}_{1,i}) + \epsilon \sum_{j=1}^{N} \mathscr{B}_{ij} G[\mathbf{x}_{1,j} - \mathbf{x}_{1,i}] - 2\eta H \mathbf{x}_{1,i},$$

$$\dot{\mathbf{x}}_{2,i} = -\dot{\mathbf{x}}_{1,i}, \quad \text{(A3)}$$

for $i = 1, 2, \ldots, N$. Considering small perturbations $\delta \mathbf{z}_i(t)$ of the ith node of layer 2, its state can be written as $\mathbf{x}_{2,i}(t) = -\mathbf{x}_{1,i}(t) + \delta \mathbf{z}_i(t)$. Then, linearizing this layer around the interlayer antisynchronization state $\mathbf{x}_{1,i}(t)$, we obtain the error associated to the dynamics transverse to the interlayer antisynchronization manifold as

$$\delta \dot{\mathbf{z}}_i = \dot{\mathbf{x}}_{1,i} + \dot{\mathbf{x}}_{2,i}$$

$$= f(\mathbf{x}_{1,i}) + \epsilon \sum_{j=1}^{N} \mathscr{B}_{ij} G[\delta \mathbf{z}_j - \delta \mathbf{z}_i] + f(-\mathbf{x}_{1,i} + \delta \mathbf{z}_i)$$

$$= Jf(\mathbf{x}_{1,i}) \delta \mathbf{z}_i - \epsilon \sum_{j=1}^{N} \mathscr{L}_{ij} G \delta \mathbf{z}_j, \quad \text{(A4)}$$

for all $i = 1, 2, \ldots, N$. Here, $Jf(\mathbf{x}_{1,i}) = \frac{\partial f(\mathbf{x})}{\partial \mathbf{x}}|_{\mathbf{x}=\mathbf{x}_{1,i}}$, and $\mathbf{x}_{1,i}$ is the dynamics of the interlayer antisynchronization state which satisfies Eq. (A3). Since all these error components are linearly independent, all the state variables of the master stability equation [Eq. (A4)] evolve transverse to the interlayer

antisynchronization subspace. Therefore, the Lyapunov exponents of the above Eq. (A4) are all transverse to $\mathcal{S}$.

Under this framework, we investigate the local stability of the interlayer antisynchronization state of a multiplex network of SL oscillators. We will verify the transition point from desynchronization to interlayer antisynchronization state through the maximum transverse Lyapunov exponent. For such multiplex network, the transverse error equation can be written as

$$\delta \dot{x}_i = \left(1 - 3x_i^2 - y_i^2\right)\delta x_i - (2x_i y_i + \omega)\delta y_i - \epsilon \sum_{j=1}^{N} \mathcal{L}_{ij}\delta x_j,$$

$$\delta \dot{y}_i = (-2x_i y_i + \omega)\delta x_i + \left(1 - x_i^2 - 3y_i^2\right)\delta y_i - \epsilon \sum_{j=1}^{N} \mathcal{L}_{ij}\delta y_j.$$

$$(A5)$$

Here, (x_i, y_i), $i = 1, 2, \ldots, N$, is the state variable of the interlayer antisynchronization manifold which dominates the evolution equation

$$\dot{x}_i = \left(1 - x_i^2 - y_i^2\right)x_i - \omega y_i - \epsilon \sum_{j=1}^{N} \mathcal{L}_{ij}x_j - 2\eta x_i,$$

$$\dot{y}_i = \left(1 - x_i^2 - y_i^2\right)y_i + \omega x_i - \epsilon \sum_{j=1}^{N} \mathcal{L}_{ij}y_j - 2\eta y_i. \quad (A6)$$

We compute the $2N$ Lyapunov exponents by solving the linearized Eq. (A5) along with the equation of motion [Eq. (A6)] of the interlayer antisynchronization state. Among them, the maximum Lyapunov exponent $\Lambda_{\max}$ as a function of ϵ and η gives the necessary condition for the local stability of this state. We will achieve interlayer antisynchronization by adjusting these two parameters (ϵ and η) so that $\Lambda_{\max}$ is less than zero.

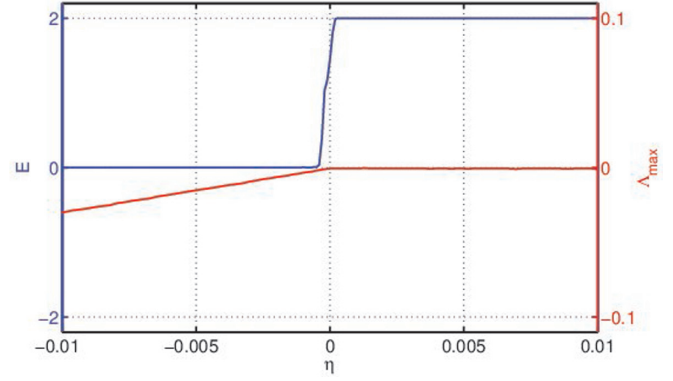FIG. 12. Stability of the interlayer antisynchronization manifold. Synchronization error E (blue line) and the largest Lyapunov exponent $\Lambda_{\max}$ (red line) of the error transverse to the interlayer antisynchronization manifold as a function of the interlayer coupling strength η. The multiplex network architecture is shown in Fig. 1(a), with each node containing a SL oscillator with $\epsilon = 0.01$ and $\omega = 3.0$.

In Fig. 12, the blue curve represents the variation of the interlayer antisynchronization error E as a function of the interlayer coupling strength η. Here, the frequency of the SL oscillators is set to $\omega = 3.0$ and the intralayer coupling strength is fixed at $\epsilon = 0.01$. For the numerical simulations we have chosen $t = 2000$ and $t_1 = 1000$ [see Eq. (A2)]. Starting with a nonzero value, E decreases and eventually drops down to zero for $\eta = -0.0013$, indicating the emergence of interlayer antisynchronization for the chosen values of ϵ and ω. At the same time, the red curve represents the variation of $\Lambda_{\max}$ with respect to η. We can observe how $\Lambda_{\max}$ descends to zero at the point where E becomes zero, indicating that our analytical local stability condition agrees well with the numerical simulations.

[1] S. Boccaletti, G. Bianconi, R. Criado, C. I. Del Genio, J. Gómez-Gardenes, M. Romance, I. Sendina-Nadal, Z. Wang, and M. Zanin, Phys. Rep. **544**, 1 (2014).

[2] M. E. Dickison, M. Magnani, and L. Rossi, *Multilayer Social Networks* (Cambridge University Press, Cambridge, 2016).

[3] S. Gomez, A. Diaz-Guilera, J. Gomez-Gardenes, C. J. Perez-Vicente, Y. Moreno, and A. Arenas, Phys. Rev. Lett. **110**, 028701 (2013).

[4] A. Cardillo, J. Gómez-Gardenes, M. Zanin, M. Romance, D. Papo, F. Del Pozo, and S. Boccaletti, Sci. Rep. **3**, 1344 (2013).

[5] M. Kivelä, A. Arenas, M. Barthelemy, J. P. Gleeson, Y. Moreno, and M. A. Porter, J. Complex Networks **2**, 203 (2014).

[6] G. Bianconi, *Multilayer Networks: Structure and Function* (Oxford University Press, Oxford, 2018).

[7] R. G. Morris and M. Barthelemy, Phys. Rev. Lett. **109**, 128703 (2012).

[8] D. Helbing, Rev. Mod. Phys. **73**, 1067 (2001).

[9] Z. Wang, L. Wang, A. Szolnoki, and M. Perc, Eur. Phys. J. B **88**, 124 (2015).

[10] S. Nag Chowdhury, S. Kundu, M. Duh, M. Perc, and D. Ghosh, Entropy **22**, 485 (2020).

[11] Y.-Z. Chen, Z.-G. Huang, H.-F. Zhang, D. Eisenberg, T. P. Seager, and Y.-C. Lai, Sci. Rep. **5**, 17277 (2015).

[12] I. Hernandez-Fajardo and L. Dueñas-Osorio, Reliability Eng. Syst. Safety **111**, 260 (2013).

[13] J. Sanz, C.-Y. Xia, S. Meloni, and Y. Moreno, Phys. Rev. X **4**, 041005 (2014).

[14] C. Granell, S. Gómez, and A. Arenas, Phys. Rev. Lett. **111**, 128701 (2013).

[15] A. Saumell-Mendiola, M. Á. Serrano, and M. Boguná, Phys. Rev. E **86**, 026106 (2012).

[16] G. Bianconi and S. N. Dorogovtsev, Phys. Rev. E **89**, 062814 (2014).

[17] J. Gao, S. V. Buldyrev, H. E. Stanley, and S. Havlin, Nat. Phys. **8**, 40 (2012).

[18] A. Pikovsky, J. Kurths, M. Rosenblum, and J. Kurths, *Synchronization: A Universal Concept in Nonlinear Sciences*, Vol. 12 (Cambridge University Press, Cambridge, 2003).

[19] S. Nag Chowdhury, S. Majhi, D. Ghosh, and A. Prasad, Phys. Lett. A **383**, 125997 (2019).

[20] S. Strogatz, *Sync: The Emerging Science of Spontaneous Order* (Penguin, London, 2004).

[21] S. Nag Chowdhury and D. Ghosh, Europhys. Lett. **125**, 10011 (2019).

[22] V. H. P. Louzada, N. A. M. Araújo, J. S. Andrade, and H. J. Herrmann, Sci. Rep. **3**, 3289 (2013).

[23] V. A. Maksimenko, V. V. Makarov, B. K. Bera, D. Ghosh, S. K. Dana, M. V. Goremyko, N. S. Frolov, A. A. Koronovskii, and A. E. Hramov, Phys. Rev. E **94**, 052205 (2016).

[24] S. Majhi, M. Perc, and D. Ghosh, Chaos: An Interdisciplinary Journal of Nonlinear Science **27**, 073109 (2017).

[25] S. Kundu, S. Majhi, and D. Ghosh, Eur. Phys. J.: Spec. Top. **228**, 2429 (2019).

[26] S. Majhi, T. Kapitaniak, and D. Ghosh, Chaos: An Interdisciplinary J. Nonlin. Sci. **29**, 013108 (2019).

[27] X. Zhang, S. Boccaletti, S. Guan, and Z. Liu, Phys. Rev. Lett. **114**, 038701 (2015).

[28] P. Khanra, P. Kundu, C. Hens, and P. Pal, Phys. Rev. E **98**, 052315 (2018).

[29] S. Jalan, A. Kumar, and I. Leyva, Chaos: An Interdisciplinary J. Nonlin. Sci. **29**, 041102 (2019).

[30] L. V. Gambuzza, M. Frasca, and J. Gomez-Gardeñes, Europhys. Lett. **110**, 20010 (2015).

[31] S. Rakshit, B. K. Bera, E. M. Bollt, and D. Ghosh, SIAM J. Appl. Dyn. Syst. **19**, 918 (2020).

[32] B. K. Bera, S. Rakshit, and D. Ghosh, Eur. Phys. J.: Spec. Top. **228**, 2441 (2019).

[33] R. Sevilla-Escoboza, I. Sendiña-Nadal, I. Leyva, R. Gutiérrez, J. Buldú, and S. Boccaletti, Chaos **26**, 065304 (2016).

[34] I. Leyva, R. Sevilla-Escoboza, I. Sendiña-Nadal, R. Gutiérrez, J. M. Buldú, and S. Boccaletti, Sci. Rep. **7**, 45475 (2017).

[35] S. Rakshit, B. K. Bera, and D. Ghosh, Phys. Rev. E **101**, 012308 (2020).

[36] I. Leyva, I. Sendiña-Nadal, R. Sevilla-Escoboza, V. P. Vera-Avila, P. Chholak, and S. Boccaletti, Sci. Rep. **8**, 8629 (2018).

[37] S. Jalan and A. Singh, Europhys. Lett. **113**, 30002 (2016).

[38] S. G. Horovitz, A. R. Braun, W. S. Carr, D. Picchioni, T. J. Balkin, M. Fukunaga, and J. H. Duyn, Proc. Natl. Acad. Sci. USA **106**, 11376 (2009).

[39] D. Mantini, M. G. Perrucci, C. Del Gratta, G. L. Romani, and M. Corbetta, Proc. Natl. Acad. Sci. USA **104**, 13170 (2007).

[40] J. R. Simpson, A. Z. Snyder, D. A. Gusnard, and M. E. Raichle, Proc. Natl. Acad. Sci. USA **98**, 683 (2001).

[41] M. Corbetta and G. L. Shulman, Nat. Rev. Neurosci. **3**, 201 (2002).

[42] M. D. Fox, A. Z. Snyder, J. L. Vincent, M. Corbetta, D. C. Van Essen, and M. E. Raichle, Proc. Natl. Acad. Sci. USA **102**, 9673 (2005).

[43] D. Li and C. Zhou, Front. Syst. Neurosci. **5**, 100 (2011).

[44] G. Deco, V. Jirsa, A. R. McIntosh, O. Sporns, and R. Kötter, Proc. Natl. Acad. Sci. USA **106**, 10302 (2009).

[45] M. Sebek, Y. Kawamura, A. M. Nott, and I. Z. Kiss, Philos. Trans. R. Soc. London A **377**, 20190095 (2019).

[46] S. N. Chowdhury, D. Ghosh, and C. Hens, Phys. Rev. E **101**, 022310 (2020).

[47] R. Karnatak, R. Ramaswamy, and U. Feudel, Chaos Solitons Fractals **68**, 48 (2014).

[48] B. Li, Nonlinear Dyn. **76**, 1603 (2014).

[49] B. K. Bera, C. Hens, and D. Ghosh, Phys. Lett. A **380**, 2366 (2016).

[50] A. Mishra, C. Hens, M. Bose, P. K. Roy, and S. K. Dana, Phys. Rev. E **92**, 062920 (2015).

[51] Q. Wang, G. Chen, and M. Perc, PLoS One **6**, e15851 (2011).

[52] S. Dixit and M. D. Shrimali, Chaos **30**, 033114 (2020).

[53] S. Majhi, S. Nag Chowdhury, and D. Ghosh, Europhys. Lett. **132**, 20001 (2020).

[54] C. R. Hens, P. Pal, S. K. Bhowmick, P. K. Roy, A. Sen, and S. K. Dana, Phys. Rev. E **89**, 032901 (2014).

[55] X.-J. Tian, X.-P. Zhang, F. Liu, and W. Wang, Phys. Rev. E **80**, 011926 (2009).

[56] C. R. Hens, O. I. Olusola, P. Pal, and S. K. Dana, Phys. Rev. E **88**, 034902 (2013).

[57] S. Nag Chowdhury, S. Majhi, M. Ozer, D. Ghosh, and M. Perc, New J. Phys. **21**, 073048 (2019).

[58] S. Nag Chowdhury, S. Majhi, and D. Ghosh, IEEE Trans. Network Sci. Eng. **7**, 3159 (2020).

[59] Y. Maistrenko, B. Penkovsky, and M. Rosenblum, Phys. Rev. E **89**, 060901(R) (2014).

[60] K. Sathiyadevi, V. Chandrasekar, and D. Senthilkumar, Phys. Rev. E **98**, 032301 (2018).

[61] K. Sathiyadevi, V. K. Chandrasekar, D. Senthilkumar, and M. Lakshmanan, Phys. Rev. E **97**, 032207 (2018).

[62] Y. Kuramoto, *Chemical Oscillations, Waves, and Turbulence* (Dover, New York, 2003).

[63] A. S. Asratian, T. M. Denley, and R. Häggkvist, *Bipartite Graphs and their Applications*, Vol. 131 (Cambridge University Press, Cambridge, 1998).

[64] S. Rakshit, B. K. Bera, J. Kurths, and D. Ghosh, Proc. R. Soc. London, Ser. A **475**, 20190460 (2019).

[65] P. Erdos and A. Renyi, Publ. Math. Debrecen **6**, 290 (1959).

[66] E. N. Gilbert, Ann. Math. Stat. **30**, 1141 (1959).

[67] T. P. Vogels and L. Abbott, Nat. Neurosci. **12**, 483 (2009).

[68] J. Soriano, M. R. Martínez, T. Tlusty, and E. Moses, Proc. Natl. Acad. Sci. USA **105**, 13758 (2008).

[69] M. De Domenico, Giga Science **6**, gix004 (2017).

[70] J. M. Buldú and M. A. Porter, Network Neurosci. **2**, 418 (2018).

[71] L. M. Pecora and T. L. Carroll, Phys. Rev. Lett. **80**, 2109 (1998).

[72] L. Tang, X. Wu, J. Lü, J.-a. Lu, and R. M. D'Souza, Phys. Rev. E **99**, 012304 (2019).